2023 IEEE/ASME International Conference on Advanced Intelligent Mechatronics (AIM)
June 28-30, 2023. Seattle, Washington, USA

Soft Continuum Robot Airbag Integrated with Passive Walker for Fall Mitigation

Jacob Thompson[1] and Ian D. Walker[1]

***Abstract*— We describe the design and prototype development of a soft continuum robotic airbag system, to be deployed from a passive walker. The system can deploy in multiple configurations: to the front, left, or right of the walker depending on the direction of a detected fall. The airbag is inflated in real time using a novel compression system. Results of experiments with the prototype are presented. The system deploys consistently across falls, significantly reducing the g-force of impact.**

I. INTRODUCTION

Falls are the second leading cause of injury deaths worldwide [1], and the leading cause of injury and death in older adults in the United States [2]. In 2018, 27.5% of U.S. adults aged 65 years or over reported at least one fall in the past year (35.6 million falls). Over 10% (8.4 million) reported a fall-related injury, resulting in an estimated 3 million emergency department visits, more than 950,000 hospitalizations, and approximately 32,000 deaths [3]. More than 95% of hip fractures are caused by falls [2]. Fear of falls has been found to be a significant risk factor limiting activity in the elderly [4].

Falls are more likely, and often more critical, for those individuals who are fragile and use walkers. In a recent study, it was found that people using a walker were 7 times more likely to be injured by a fall compared to those using a cane [5]. Passive walkers help provide stability for such individuals during ambulation, but offer no protection in the event of a fall. This paper discusses the augmentation of a passive walker with a robotic airbag system to mitigate the effect of falls.

The concept of creating robotic versions of passive walkers, or "smart walkers", is not new. An early smart walker was a modified rollator walker developed by the Dublin Institute of Technology using hydraulic disc brakes [6]. This system used a high-speed linear actuator to vary the pressure on the braking disk. The brake activated if the user moved too fast or if the walker sensed the user wanted to stop. Another rollator walker with pneumatic brakes on the wheels [7] simulated three different falling situations - freezing of limbs, stumble, and loss of balance. Another walker that implements fall prevention is the RT Walker [8], which focuses on calculating the user's center of gravity in real time. When the user's center of gravity is detected to be outside the region of stability, brakes are enabled. One drawback of these braking systems is that they do not address cases when the walker is tilting or falling to the left or the right.

[1]The authors are with the Department of Electrical and Computer Engineering, Clemson University, Clemson, SC 29634, USA. jat5@g.clemson.edu, iwalker@g.clemson.edu

Some smart walkers aim to help the user in a more subtle way. A robotic walker developed by the Japan Advanced Institute of Science and Technology (JAIST) autonomously adjusts its direction and speed according to the user's walking movements [9]. It does not require any user input, instead using a pair of laser range finders to detect the user's legs and any obstacles in the environment. The walker uses a trio of Mecanum wheels to drive the walker away from obstructions in an indoor environment, while still following the general direction the user wants to go. This robotic walker provides a measure of fall prevention by avoiding obstacles or drop-offs that could unbalance the user, but in the case of a fall it simply locks up the wheels.

Several groups have worked on "human airbags" - wearable devices which deploy when the wearer is falling. These devices come in many forms such as vests, belts [10], jackets, or harnesses [11]. Helite is a company that has made wearable airbag vests for skiing [12] and cycling [13]. The Hit-Air inflatable air vest [14] is a body-worn airbag with a pull cord marketed towards equestrians where the rip cord is attached to the horse's saddle and is pulled if they fall off the horse. These commercially available products demonstrate a need for personal fall protection in a variety of environments.

Many human airbag systems for fall protection are designed as a belt or fanny pack that the user must wear all the time. For example, the system discussed in [15] involves a belt with a microcontroller, IMU, compressed CO_2 cylinder, and actuation mechanism with airbags around the user's hip. When the IMU detects the person is falling, it punctures the gas cylinder and rapidly inflates the small airbag in front of the user's hip within 333ms. A similar device is designed in [16], and built in [17].

However, these systems are static, in the sense that the deployed system remains the same regardless of the specific fall endured by the individual. In this paper, we introduce a novel alternative: the first reconfigurable (continuum) robotic airbag system featuring the ability to deploy the airbag system in the direction most needed. This provides the unique ability to tailor the response to the situation encountered, e.g. maximizing the volume of airbag between the falling individual and the environment.

Continuum (continuous backbone) robots have been the subject of much interest and research in the past few years [18]. Continuum robots have been successfully applied to a variety of medical procedures [19]. Inspired in large part by emerging research in soft robotics [20], [21], [22], researchers have been exploring the shaping of soft air-filled volumes using tendons to create continuum robots [23].

978-1-6654-7633-1/23/$31.00 ©2023 IEEE

Numerous tendon-actuated pneumatic continuum robots, e.g. [24], [25], [26], [27], [28] have been demonstrated, and the design here expands on our experience in the area [25].

The paper is organized as follows. The design concept for the soft airbag system, and its physical realization in a prototype, are described in the following section. Experiments with, and performance validation of, the prototype are reported in section III. Discussion and conclusions are presented in section IV.

II. SOFT CONTINUUM AIRBAG DESIGN AND PROTOTYPE

A. Design Concept

The key objective in this work was to develop a novel airbag deployment system, integrated with a walker, which is not static but instead robotic, i.e. with programmable configurability, varying to meet the deployment needs of a specific fall. The goal was for the airbag to be stowed in one face of the walker, but be deployable in real time, as a function of the direction of a detected fall, across the range of a semi-cylindrical region from the left side of, around the front of, and to the right side of, the walker.

In order to address the above specifications, the core element of the design selected was an inflatable continuum arm, actuated (configured) in real time by remotely actuated tendons. A second novel design choice lay in the method adopted to inflate the airbag. We elected to use a partly pre-inflated fabric volume, and suitably compress a "reservoir" bladder element of it to quickly inflate a continuum robot arm element of it. The details of the realized design are presented in the following section.

B. Prototype Development

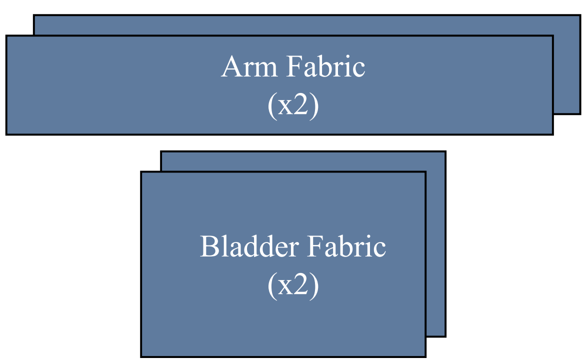

Fig. 1: Identical fabric pieces cut out for the arm (top) and bladder (bottom)

1) Arm and Bladder Construction: The fabric portion of the system was constructed out of Heat Sealable 200 Denier Oxford Nylon. This material was chosen because in an earlier inflatable continuum arm development [26] it could withstand the most pressure of all the materials tested. The fabric has a coating on one side similar to a very thin layer of hot glue. When two layers of the fabric are laid on top of each other so that each glue-layer side is facing each other, a soldering iron can be used to seal them together for a very tight seal. We found that a temperature of 240°C paired with a large knife-style soldering iron tip worked best for sealing the sheets of fabric together.

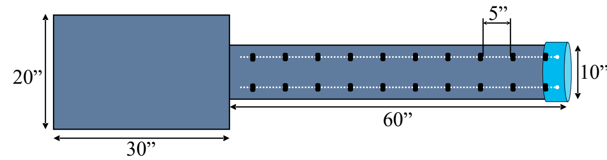

Fig. 2: Relative dimensions and positions of fabric arm components

The fabric assembly of the project was made of two parts - the arm and the air bladder, each of which was made from two identical cuts of fabric as shown in Figure 1. The arm was made from two pieces that were 152cm by 50cm (60in by 20in), and the bladder was made with two pieces that were 76cm by 51cm (30in by 20in) (Figure 2). These dimensions included a 1 inch margin on the outside edges for sealing the pieces together.

An air nozzle from an inflatable stick was added to the arm to provide a convenient way to increase or decrease the amount of air in the system between tests. The same soldering iron heat-sealing technique was used as on the rest of the arm, with the adhesive side of the fabric pressed against the tube fabric. The nozzle was attached before flipping the arm inside out.

Fig. 3: First full inflation of the fabric arm and air bladder

The arm was flipped inside out so that the adhesive coated side was facing outwards, while the air bladder had the adhesive coating on the inside. The arm slid inside the air bladder and was sealed in place with the same soldering iron sealing method. The assembled bladder and arm can be seen inflated in Figure 3.

Fig. 4: Components of the end of the arm

2) Integration of Tendons: In order to enable shape controllability of the arm, numerous 3D printed parts were attached to the bladder as shown in Figures 2 and 4. The arm featured 32 individual cable guides printed in black PLA filament. A 64cm (25") long thin strap 3D printed with flexible black NinjaFlex filament was passed through slots in the arm holding the cable guides in place. A "crown" was located at the end of the arm where all four cables are attached. The crown was printed in semi-flexible SainSmart TPU filament. This was also held in place with a flexible strap through strap guides. Eight rows of cable guides were spaced every 14.2mm (5.6"), leaving 12.7cm (5") between each cable guide. A a 6.4cm (2.5") section of spiral cable wrap was added between each cable guide to improve the bending consistency of the arm.

3) Walker and Actuators: The system was integrated within a Drive Medical 10210-1 Deluxe 2-Button Folding Walker with Wheels [29]. This walker was chosen because it was commonly used (more than 20,000 Amazon reviews).

We considered several different deployment methods including volume displacement, CO_2, high pressure air (HPA), and vehicle airbags. Each of these methods have their own merits, but each had significant drawbacks for the prototyping of a continuum system. Using CO_2 canisters would have cost around \$8 per deploy, and it would have been challenging to make a system that perfectly inflated upon cartridge puncture but that did not over-inflate (and explode) or under-inflate (and not effectively catch the user). Similar issues exist with HPA, along with concerns of the time required to release a sufficient volume of HPA into the arm. Airbag cartridges are very dangerous, produce toxic chemicals, and expensive (\$200+ per deploy).

Consequently, we selected a method of inflation based on volume displacement. We planned to construct one section that would hold the air before the system deployed, and have that section be continuous with the arm section of the system. The arm would deploy when air was pushed from one place to another inside the sealed container. This rapid volume-displacement inflation method is unique among continuum robotics systems and smart walker systems. The volume of air in our arm is 1.50 ft^3 so to inflate the arm in half a second it takes $1.50\ \text{ft}^3/0.5s = 3.0\ \text{ft}^3/s$ or 180 cubic feet per minute (CFM).

The inflation system's method of actuation was based on a R860054 brushless drill [30] which spins a shaft that wraps up the nylon webbing straps to squeeze air from the bladder into the arm. The drill was mounted to a 3D printed plate with six zip ties.

The next step was to integrate the straps with the drill and bladder/arm. The main spinning shaft was a 3/4" square aluminum rod. Each webbing strap was held in place by two 3D printed pieces mounted on the square rod. These pieces were round on the outside, effectively turning the square shaft into a 40mm (1.6") round tube. M4 bolts were passed through the printed piece, webbing strap, and into a threaded hole in the aluminum square shaft. The two mounting holes in the webbing strap were made by pressing a hot soldering iron to the webbing strap, forming a 5mm hole with melted edges that prevented fraying.

There was a "bearing" between every two webbing straps, which consisted of a 3D printed part that was square on the inside and round on the outside. This bearing helped distribute the forces on the rod and minimized the deflection of the rod. A small amount of SuperLube Synthetic Multi-Purpose Grease was applied to each bearing after installation. The rod assembly was attached to the main plate by several 3D printed mounts.

Front and rear views of the final overall system are shown in Figures 5 and 6. Along with the mechanical components discussed previously, the figures show several boxes which hold electrical components of the system.

Each steel cable tendon was stored in a cable spool on a stepper motor shaft. Dual-shaft NEMA 17 stepper motors and AMT102-V rotary encoders were attached to the front of the same mount. An electromagnetic stepper motor brake was mounted to the rear side of each stepper motor. A stainless steel flange adapter was connected to the motor shaft, and the cable spool assembly was mounted to the flange adapter.

This motor and spool assembly was then mounted to the outside of an arm ring using M4 bolts. The arm ring had an internal path that guided the cable from vertical to horizontal. The arm ring mounted to an angled plate that was offset from the walker to provide an adequate bending radius for the fabric of the arm.

4) Electrical System: The prototype was completely untethered - everything ran off batteries, and all required electronics were mounted on the walker frame. A Teensy 4.1 microcontroller was used as the controller. The system was powered by a 6S 22.2V 4500mAh 45C LiPo Battery. A Pololu D24V150F12 12V 15A voltage regulator stepped down the battery voltage to 12V for the stepper motor drivers.

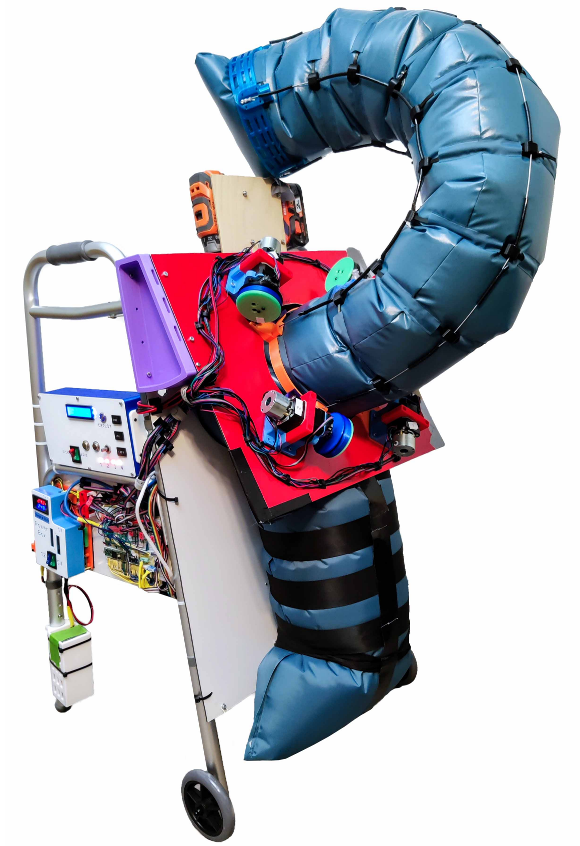

Fig. 5: Front view of the complete system. The air reservoir with the cage of straps can be seen on the bottom right portion of the image.

A Pololu D36V50F5 5V 5.5A voltage regulator provided a steady 5V for the Teensy 4.1 and a variety of other components that required 5V to function. The trigger on the drill was replaced with our own electrical components so that we could control the drill using the microcontroller.

III. EXPERIMENTS AND VALIDATION

A. Testing Procedure

The prototype described in the previous section was evaluated in a series of trials. Each trial was conducted multiple times. In each trial set, the walker was tipped forwards and to both the left and right. In each of these cases, the system was tested both with the airbag un-deployed (baseline test) and fully deployed. It was assumed throughout testing that real-time detection of the timing and direction and the falls was available. (There is a fairly extensive literature on fall detection, e.g. [31], and fall detection was not the goal of this research.) Therefore, airbag deployment was triggered manually, and the configuration deployed to was pre-selected (but, nevertheless implemented in real time) based on the timing and direction of fall imparted to the walker.

A dummy was attached to the walker using bungee cords to simulate the presence of a human user. The dummy is a 6-foot tall plastic blow-mold mannequin weighing 12 pounds. Data from both the dummy and the robot system

Fig. 6: Overview of walker rear side

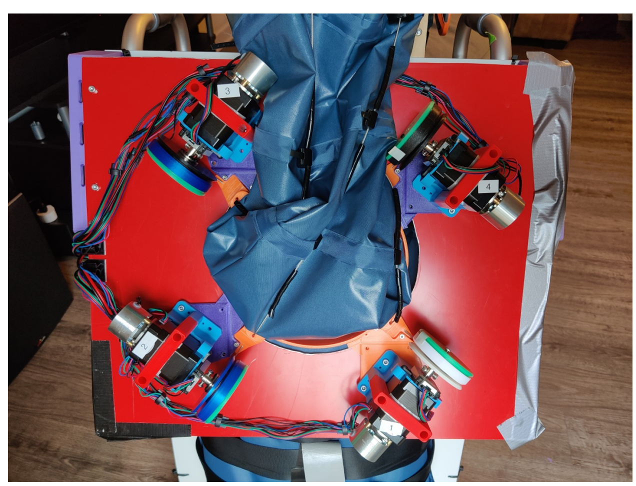

Fig. 7: All motor assemblies mounted on the walker

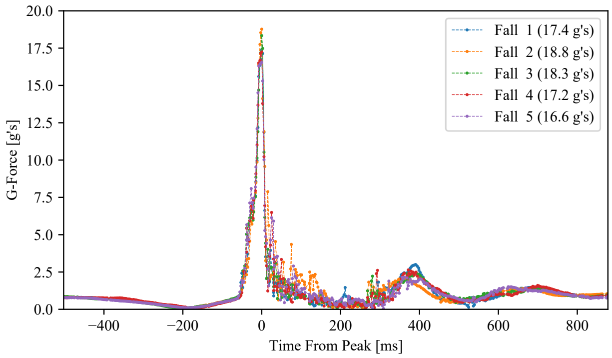

Fig. 8: Data logging - dummy

were recorded. Attached to the dummy was a cell phone running the Physics Toolbox Sensor Suite [32] measuring, among other quantities, the linear acceleration and g-force experienced by the phone. Figure 8 shows typical output, over five tests (baseline tests for walker and dummy with no deployment of airbag, in this specific instance). Note the consistency of the results across tests.

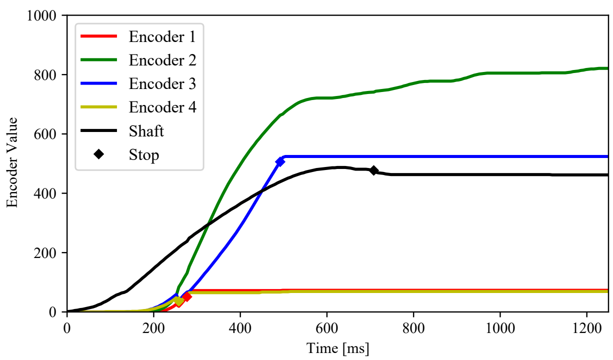

Fig. 9: Data logging - robot during left-sided fall

Each test was video recorded and key quantities sensed from the airbag system, including encoder readings and key event timings, were logged. A typical example of the data logging can be seen in Figure 9. After each cable is spooled to its desired position the associated brake is applied and the motor driver enabled to hold the tendon at that length.

For the left-sided and right-sided fall tests, the arm was augmented with a small inflatable ring. This aided in stabilizing the dummy following the fall.

B. Results and Discussion

Results of the testing demonstrated the robotic airbag system to be highly effective. The airbag consistently deployed in around 500 milliseconds, well inside the fall time of the walker. Qualitatively, the airbag was able to consistently effectively cushion the falls, in each direction. Figures 10, 11, and 12 illustrate typical cases for forward, left, and right deployments. Footage of falls is provided in the video accompanying this paper.

Fig. 10: Progression of typical deployment for forward fall

Fig. 11: Progression of typical deployment for left fall. The inflatable ring is shown in the bottom series of images.

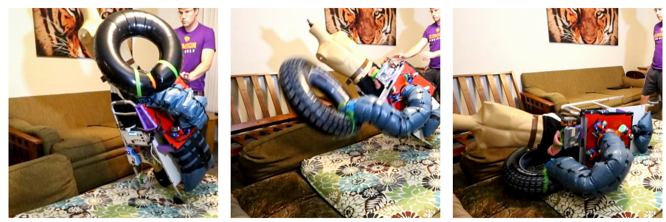

Fig. 12: Progression of typical deployment for right fall

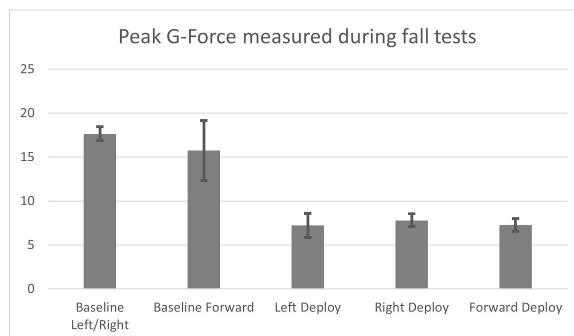

Fig. 13: Peak G-Forces measured during fall fall tests

Figure 13 summarizes overall quantitative testing results, using data from five representative tests of the system. On average, the measured maximum g-force of the deployed system in the forward falls is 46% of that for the baseline, i.e. undeployed, case. The average measured maximum g-force for the deployed system in left/right falls is 42% of that for the baseline case. The reduction in measured impact demonstrates the effectiveness of the airbag system.

IV. CONCLUSIONS

We have introduced a soft robotic airbag, whose configuration can be controlled in real time to deploy in the direction of a forward or sideways fall. The core of the robotic airbag system is an air-filled, tendon-configured, continuum arm-like structure. The airbag is integrated into a conventional passive walker. A novel single motor system is used to deploy the airbag by transferring air from a reservoir into the arm in real time. Tests with a prototype demonstrate the effectiveness of the system in deploying through the desired range of configurations. The g-forces of impact are significantly and consistently reduced, across the configuration space of the system.

We are currently investigating alternative geometries for the deployed airbag, as well as optimization of the number and arrangement of tendons configuring the airbag. Future work includes the integration of real-time fall detection and its triggering of automatic airbag deployment, along with testing with human subjects.

ACKNOWLEDGMENT

This work was sponsored in part by the U.S. National Science Foundation under NRI grants 1924721 and 2221126.

REFERENCES

[1] World Health Organization, "Falls", https://www.who.int/news-room/fact-sheets/detail/falls, accessed October 18, 2021.

[2] Centers for Disease Control and Prevention, "Keep on Your Feet: Preventing Older Adult Falls", https://www.cdc.gov/injury/features/older-adult-falls/index.html, accessed October 18, 2021.

[3] B. Moreland, R. Kakara, and A. Henry, "Trends in Nonfatal Falls and Fall-Related Injuries Among Adults Aged $\geq$ 65 Years — United States, 2012–2018", CDC Weekly, 69(27), July 10, 2020, pp. 875–881.

[4] J.E. Walker and J. Howland, "Falls and Fear of Falling Among Elderly Persons Living in the Community: Occupational Therapy Interventions", American Journal of Occupational Therapy, Vol. 45(2), 1991, pp. 119-122.

[5] C. Eustice, "Elderly Falls Tied to Canes and Walkers", April 3, 2020, https://www.verywellhealth.com/elderly-falls-tied-to-canes-and-walkers-2552063, accessed 18 October, 2021.

[6] E. Coyle, A. O'Dwyer, E. Young, K. Sullivan and A. Toner, "Controlled Breaking Scheme for a Wheeled Walking Aid", IFAC Workshop on Programmable Devices and Embedded Systems PDeS 2006, Brno, Czech Republic, February 14-16, 2006, pp. 21-15.

[7] M. Azqueta-Gavaldon, I. Azqueta-Gavaldon, M. Woiczinski, K. Bötzel, and E. Kraft, "Automatic Braking System and Fall Detection Mechanism for Rollators", Proceedings of the 6th ACM International Conference on Bioinformatics and Biomedical Science, Singapore, 2017, pp. 158–161.

[8] Y. Hirata, S. Komatsuda, and K. Kosuge, "Fall Prevention Control of Passive Intelligent Walker Based on Human Model", Proceedings IEEE/RSJ International Conference on Intelligent Robots and Systems (IROS), 2008, pp. 1222-1228.

[9] G. Lee, E-J. Jung, T. Ohnuma, N. Chong, and B-J Yi, "JAIST Robotic Walker Control based on a Two-layered Kalman filter", Proceedings IEEE International Conference on Robotics and Automation (ICRA), 2011, pp. 3682-3687.

[10] C.C. Weiss, "Helite's Airbag Belt Gives Wearers a Hip Check", https://newatlas.com/helite-hipair-wearable-airbag/52867/" January 2018, accessed October 11, 2021.

[11] M. Tucker, "Free Fall Tool Harness and Airbag System", https://www.behance.net/gallery/11232605/Free-Fall-Tool-Harness-and-Airbag-System" October 2013, accessed 11-October-2021.

[12] C.C. Weiss, "Helite Readies Wearable Skiing Airbag for 2014 Winter Olympics", https://newatlas.com/helite-airbag-skiing/26190/, February 2013, accessed 11-October-2021.

[13] B. Coxworth, "Airbag-equipped cycling vest instantly inflates when accidents happen", New Atlas, https://newatlas.com/helite-bsafe-airbag-cycling-vest/58050/, January 2021, accessed 11-October-2021.

[14] Hit-Air, "Hit-Air inflatable air vest SV2 model in Black Size S", https://www.amazon.com/Hit-Air-inflatable-vest-model-Black/dp/B00E40JJQ8/, 2021, accessed 11-October-2021.

[15] G. Shi, C.S. Chan, W.J. Li, K-S Leung, Y. Zou, and Y. Jin, "Mobile Human Airbag System for Fall Protection Using MEMS Sensors and Embedded SVM Classifier", IEEE Sensors Journal, Vol. 9, No. 5, 2009, pp. 495-503.

[16] J. Li, "Wearable and Controllable Protective System Design for Elderly Falling", Proceedings 6th International Conference on Mechanical Engineering and Automation Science (ICMEAS), 2020, pp. 187-194.

[17] G. Shi, C.S. Chan, Y. Luo, G. Zhang, W.J. Li, P.H. Leong, and K-S. Leung, "Development of a Human Airbag System for Fall Protection Using MEMS Motion Sensing Technology", Proceedings IEEE/RSJ International Conference on Intelligent Robots and Systems (IROS), 2006, pp. 4405-4410.

[18] D. Trivedi, C.D. Rahn, W.M. Kier, and I.D. Walker, "Soft Robotics: Biological Inspiration, State of the Art, and Future Research", Applied Bionics and Biomechanics, 5(2), pp. 99-117, 2008.

[19] J. Burgner-Kars, D.C. Rucker, and H. Choset, "Continuum Robots for Medical Applications: A Survey", IEEE Transactions on Robotics, Vol. 31, No. 6, December 2015, pp. 1261-1280.

[20] H. Lipson, "Challenges and Opportunities for the Design, Simulation, and Fabrication of Soft Robots", Soft Robotics, Vol. 1, No. 1, pp. 12-20, 2014.

[21] C. Majidi, "Soft Robotics: A Perspective – Current Trends and Prospects for the Future", Soft Robotics, Vol. 1, No. 1, pp. 2-11, 2014.

[22] S.G. Nurzaman, F. Iida, L. Margheri, and C. Laschi, "Soft Robotics on the Move: Scientific Networks, Activities, and Future Challenges", Soft Robotics, Vol. 1, No. 3, pp. 154-158, 2014.

[23] I.D. Walker, H. Choset, and G. Chirikjian, "Snake-like and Continuum Robots", Chapter 20, in Springer Handbook of Robotics, pp. 481-498, 2016.

[24] G. Immega and K. Antonelli, "The KSI Tentacle Manipulator," Proceedings IEEE International Conference on Robotics and Automation, Nagoya, Japan, pp. 3149-3154, 1995.

[25] W. McMahan, B. A. Jones, and I. D. Walker, "Design and Implementation of a Multi-section Continuum Robot: Air-Octor," Proceedings IEEE/RSJ International Conference on Intelligent Robots and Systems (IROS), Edmonton, Canada, pp. 3345-3352, 2005.

[26] P.H. Nguyen, I.I.B. Mohd, C. Sparks, F.L. Arellano, W. Zhang, and P. Polygerinos, "Soft Poly-Limbs for Physical Assistance of Daily Living Tasks", Proceedings IEEE International Conference on Robotics and Automation, Montreal, Canada, pp. 8429-8435, 2019.

[27] E.W. Hawkes, L.H. Blumenschein, J.D. Greer, and A.M. Okamura, "A Soft Robot that Navigates its Environment Through Growth", Science Robotics, Vol. 2, Issue 8, pp. 1-7, 2017.

[28] A. Marchese, K. Komorowski, C.D. Onal, and D. Rus, "Design and Control of a Soft and Continuously Deformable 2D Robotic Manipulation System", Proceedings IEEE International Conference on Robotics and Automation, Hong Kong, pp. 2189-2196, 2014.

[29] Drive Medical, Amazon, "Drive Medical 10210-1 Deluxe 2-Button Folding Walker with Wheels", 2021, https://www.amazon.com/dp/B001HOM4U2/, accessed 11-October-2021.

[30] RIDGID, "RIDGID 18-volt lithium-ion cordless brushless drill",https://www.homedepot.com/p/301853891, 2021, accessed 11-October-2021.

[31] Z. Zhong, F. Chen, Q. Zhai, Z. Fu, J.P. Ferreira, Y. Liu, J. Yi, and T. Liu, "A Real-time Pre-impact Fall Detection and Protection System", Proceedings IEEE/ASME International Conference on Advanced Intelligent Mechatronics (AIM), Auckland, New Zealand, 2018, pp. 1039-1044.

[32] Vieyra Software, "Physics Toolbox Sensor Suite", 2021, https://play.google.com/store/apps/details?id=com.chrystianvieyra .physicstoolboxsuitehl=enUSgl=US, accessed 15-October-2021.